Inter-comparison and cross-validation of tomography models – aims, scope and methods

W. Rohm (1,2), A. Geiger (3), M. Bender (4), M. Shangguan (5), H. Brenot (6), T. Manning (2)

(1) Wroclaw University of Environmental and Life Sciences, Institute of Geodesy and Geoinformatics, Wroclaw, Poland (witold.rohm@up.wroc.pl), (2) Royal Melbourne Institute of Technology, SPACE Research Center, Melbourne, Victoria, Australia, (3) ETH Zuerich, Geodesy and Geodynamics Lab, Zuerich, Switzerland, (4) Deutscher Wetterdienst, Offenbach am Main,Germany, (5) Helmholtz-Zentrum Potsdam, Deutsches GeoForschungszentrum (GFZ), Department 1.1, Potsdam, Germany, (6) Belgian Institute for Space Aeronomy, UV-vis, Brussels, Belgium

The Global Navigation Satellite Systems (GNSS) signals transmitted from satellites are subjected to atmospheric delays since the signals have to propagate through different layers of the atmosphere before GNSS receiver receives them. Two major distinctive effects according to the nature of the impact on the signal propagation are the ionosphere which is a dispersive media and the troposphere which is a non-dispersive layer.

To analyse the lower part of the atmosphere the troposphere part of the delay could be utilized as observations for GNSS tomography models. The integrated measure of the delay into direction to satellite is converted into distribution of refractivity (total or wet), or directly water vapour using Radon inverse transform. The ill – conditionedess and ill-posedness of the equations set results in complexity of the problem. Currently there exist a couple of GNSS tomography models. In order to foster best practice, resolve main issues and benefit from different approaches, IAG in the frame of Sub-Commission SC 4.3 – "Remote sensing and modelling of the atmosphere", proposes to install the Working Group "Inter-comparison and cross-validation of tomography models".

This WG intends to address the main issues dealing with GNSS tomography. Promote the inter-comparison and cross-validation of different tomography models and approaches by using same data sets over same areas. Improve GNSS tomography by the integration of new GNSS measurements aiming at an enhanced reliability of tomography results, by increasing the number of observations and by incorporating cross-sectional observations. Promote the sharing of GNSS tomography technique data, results and software. Discuss the need of a "tomography service". This paper presents initial participants (WUELS, RMIT, ETH, DWD, GFZ, and BIRA), methods and aims of the WG. It is also a call for interested groups and individuals to join this WG to help promote, use and develop GNSS tomography models.

INTRODUCTION

The GNSS signals carrier frequencies were designed to sit in microwave spectrum reserved for navigation, section L (2-1 GHz). Such spectrum's allocation is to minimize signal's distortion in atmosphere, and allow for all weather operational usage of the system. Even though 5% of the signal's way between satellite and receiver resides not in the relative vacuum, the impact of the Earth's troposphere is significant. According to Thayer (1974) is given as:

$$N_0 = k_1\frac{p-e}{T}\cdot Z_d^{-1} + \left(k_2\frac{e}{T} + k_3\frac{e}{T^2}\right)\cdot Z_v^{-1}$$

Usually researchers only focus on the GNSS signal phase speed change (delay) in the neutral atmosphere, neglecting signal bending, and not considering any effects on signal's energy. The tomography processing signal is mostly modeled as a straight line between satellite and receiver, the signal total delay STD in neutral atmosphere could be given as:

$$STD = \int N_0\cdot ds = \int N_d\cdot ds + \int N_v\cdot ds = SHD + SWD$$

Where SHD is a slant dry delay, and SWD is a slant wet delay, the tomography model utilize mainly later, to investigate water vapour distribution.

GNSS tomography is a remote sensing method which applies an inverse Radon transform on the integrated slant measurements of refractivity (total or wet). The method works in conjunction with a combination of; apriori data from a NWP model, radiosonde (RS) data, RO profiles and ground meteorological stations. Currently several groups around the world are working on the development of comprehensive tomography models, for example; ETH Zurich AWATOS model (Perler et al., 2011), GFZ Potsdam (Bender et al., 2011), WUELS Wroclaw (Rohm et al., 2011), BIRA Brussels (Brenot et al., 2012). The number of unknowns, is in principle larger than number of scanning rays and unlike in other tomography applications scanning is only possible from horizontal angles limited by the cut off angle function. Thus most of the time tomography equation reads as follows:

$$SWD^T = A\cdot N_v$$

is ill-conditioned and ill-posed. Therefore matrix's A inversion is a central problem of all GNSS tomography applications.

STANDARD GNSS TOMOGRAPHY PROCESSING

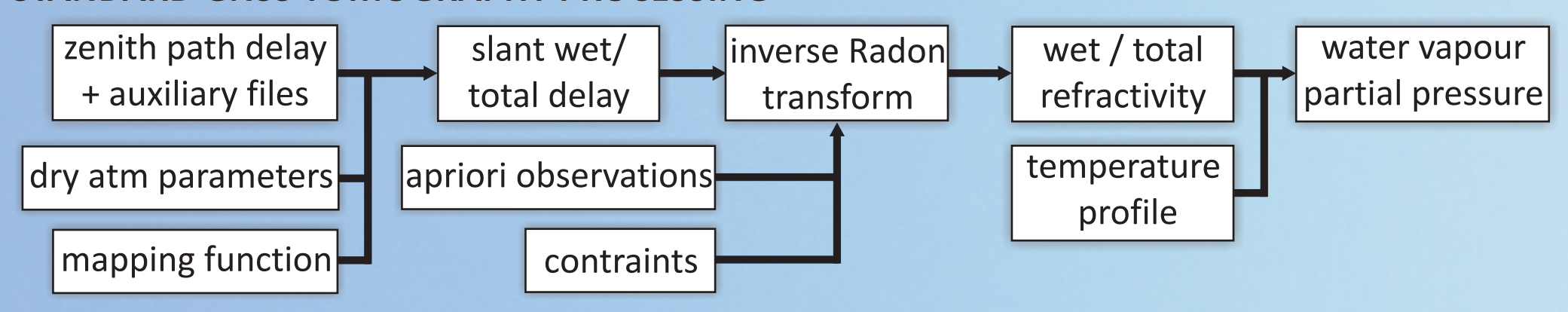
zenith path delay + auxiliary files
dry atm parameters
mapping function
slant wet/ total delay
apriori observations
contraints
inverse Radon transform
wet / total refractivity
temperature profile
water vapour partial pressure

TOMO2 MODEL

The model developed in the Wroclaw University of Environmental and Life Sciences, currently also used in RMIT University has undergone major upgrades to the underlying algorithm to facilitate the severe weather monitoring capabilities. The new features include:

- the use of Kalman filters instead of ordinary least squares to obtain estimates of wet refractivity

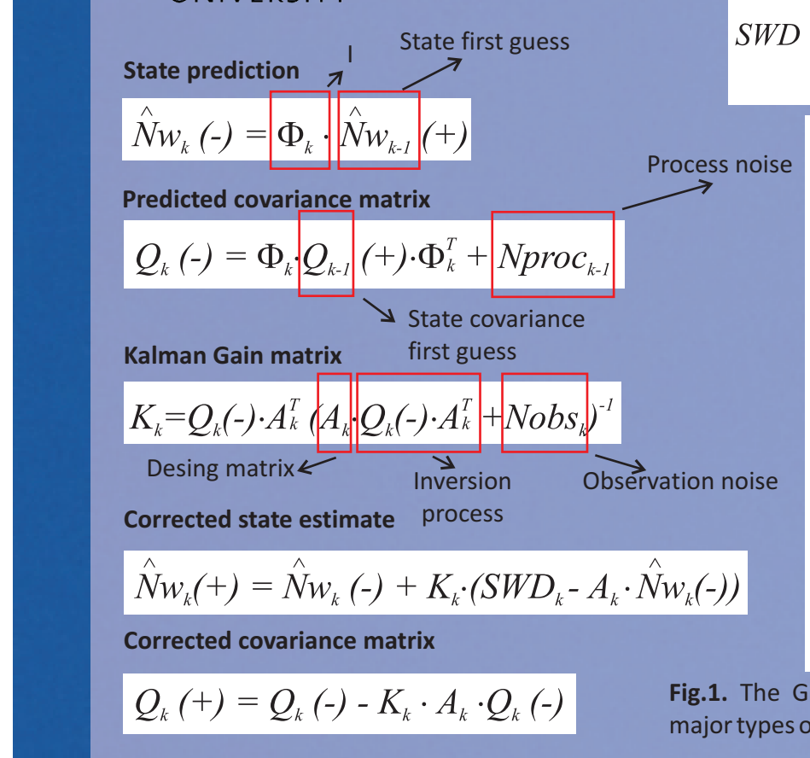
State prediction

$$\hat{N}w_k(-) = \Phi_k\cdot\hat{N}w_{k-1}(+)$$

Predicted covariance matrix

$$Q_k(-) = \Phi_k\cdot Q_{k-1}(+)\cdot\Phi_k^T + Nproc_{k-1}$$

Kalman Gain matrix

$$K_k = Q_k(-)\cdot A_k^T\,(A_k\cdot Q_k(-)\cdot A_k^T + Nobs_k)^{-1}$$

Corrected state estimate

$$\hat{N}w_k(+) = \hat{N}w_k(-) + K_k\cdot(SWD_k - A_k\cdot\hat{N}w_k(-))$$

Corrected covariance matrix

$$Q_k(+) = Q_k(-) - K_k\cdot A_k\cdot Q_k(-)$$

$$SWD = A\cdot N_w \;\Rightarrow\; \begin{bmatrix} SWD \\ N_{wapriori} \\ 0 \end{bmatrix} = \begin{bmatrix} A \\ A_{apriori} \\ W \end{bmatrix}\cdot N_w$$

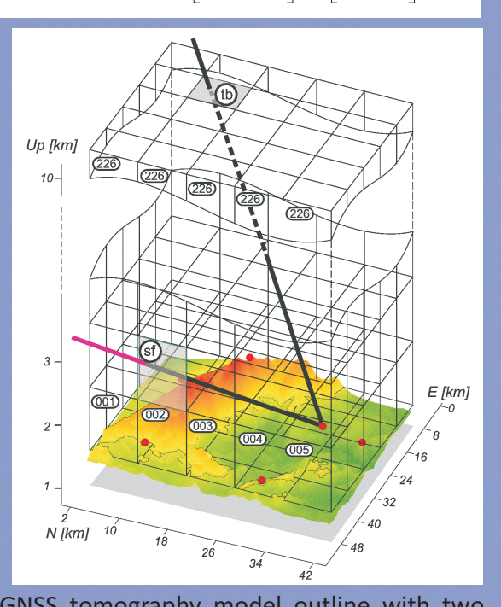

Fig.1. The GNSS tomography model outline with two major types of signal side face(sf) and top boundary (tb).

The model state, wet or total refractivity is modelled as a random walk process with some additional process noise (Nproc), the amplitude of the noise is empirically set up to 3 mm/km/ per 0.5 h of wet refractivity. The observations (SWD) update the model state according to a Kalman gain matrix, subjected to the observation noise (Nobs). The noise settings reflect previous findings in error propagation in GNSS troposphere estimates and the latest ray tracing retrievals. The noise values are strongly elevation dependent and noticeably decrease in the range of 0.005 to 0.05 m. The estimation step is consistent with SWD time resolution, thus an update of the model state is performed every 30 minutes (Australia) or 60 minutes (Poland).

- model nesting to take into account signal from low level satellites and flexible setting of voxel number in north and east direction

The actual extent of the model domain depends on the GNSS CORS network setup and the number of voxels in north and east directions. The model takes into account the elevation cut-off angle setting, to make sure all observations into the direction of the satellite (SWD) are contained inside the voxel model, so that there are no large errors, resulting from a signal leaving the model from a side surface.

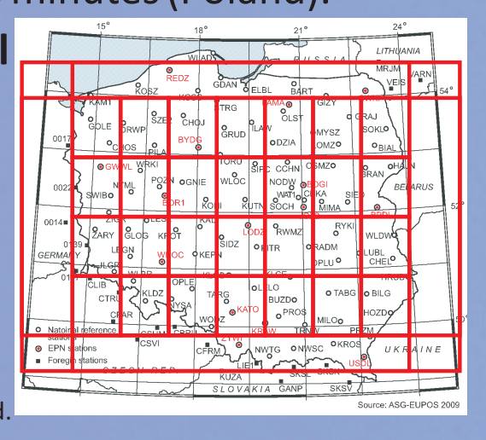

Fig.2. Horizontal model setup for Poland.

- flexible setting of layer thickness in vertical direction

The exponential decrease in water vapour content in the atmosphere presents feasible research possibilities of splitting the troposphere into several layers. The bottom part of the troposphere where the water vapour content is greatest is split into layers of finer thickness, while the upper troposphere, due to its lower moisture content and sensitivity limitations of GNSS tomography, is divided into more coarse layers.

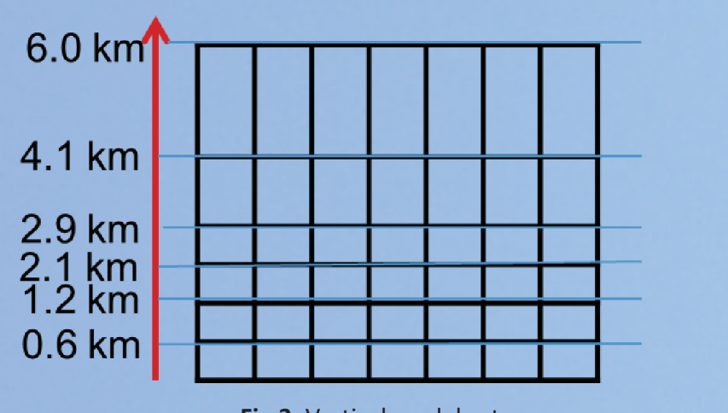

Fig.3. Vertical model setup.

- robust estimation

GNSS tomography in our application (without implicit constraints) is prone to the noise in data, therefore robust algorithm is set on the observations, and then based on SVD on covariance matrix of estimated process, downweighting the outlayers in observations and in outputs.

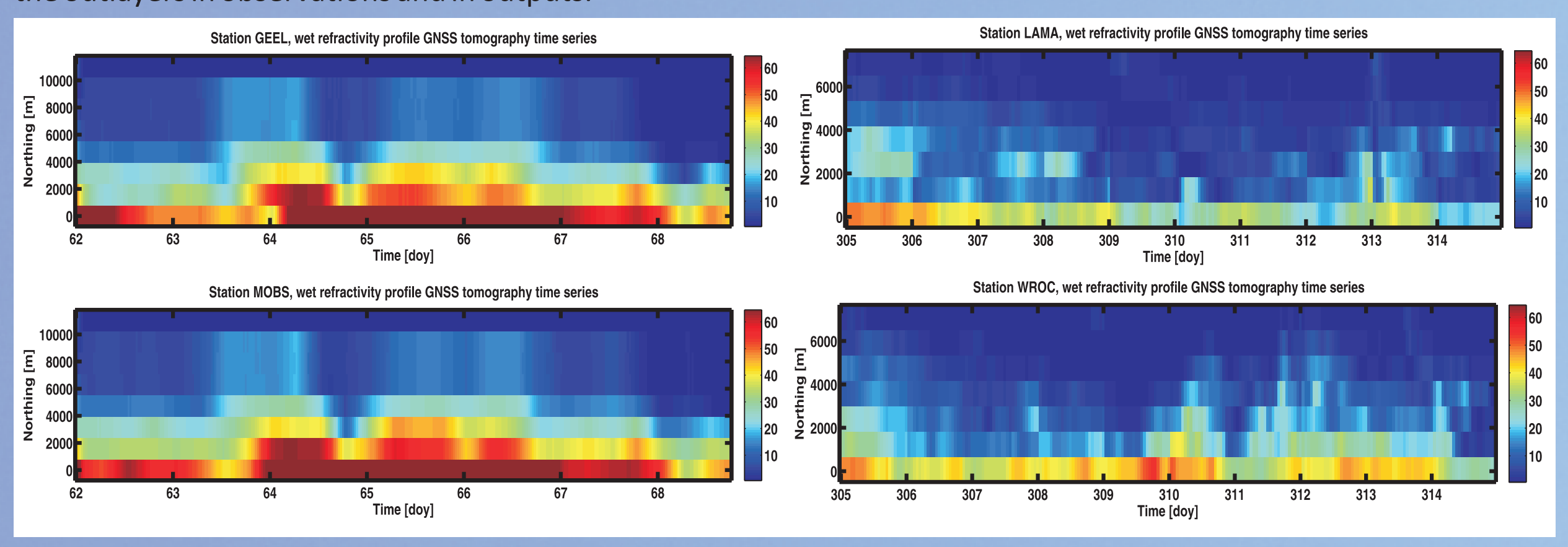

Fig. 4. The wet refractivity model crossection at the station GEEL, MOBS, LAMA, WROC

AWATOS2 MODEL

This model has been developed at the Swiss Federal Institute of Technology Zurich (ETH Zurich) for the recent 10 years. It is currently also in use at RMIT University and proved to be a reliable and useful tool for studying the troposphere conditions.

Observations

The Bernese GPS processing software V5.0 is used to attain the Zenith Total Delays (ZTD) and the DD residuals $\Delta\Phi_{a,b}^{x,y}$ using a shortest distance baseline strategy and a double differencing approach (Dach et al, 2007). A double difference path delay observation can be reconstructed between 2 satellites (x and y) and 2 receivers (a and b) using the ZTDs from the receivers which are mapped to the corresponding elevations of the satellites using the Niell mapping function (Niell 1996) $m(el_{rec}^{sat})$ with the addition of DD residuals. In case the wet refractivity is of interests, the dry component of atmosphere is eliminated with high accuracy using additional ground meteorological observations at the GPS station using the dry Saastamoinen model (Saastamoinen 1972). The final DD SWD equation (Troller et al., 2006) reads as follows:

$$\Delta^{2,SWD\,x,y}_{a,b} = \overline{\Delta^{2,SWD\,x,y}_{a,b}} + \Delta\Phi^{x,y}_{a,b}$$

where

$$\overline{\Delta^{2,SWD\,x,y}_{a,b}} = (\overline{\Delta^{ZWD}_{b}}\cdot m(el^x_b) - \overline{\Delta^{ZWD}_{a}}\cdot m(el^x_a)) - (\overline{\Delta^{ZWD}_{b}}\cdot m(el^y_b) - \overline{\Delta^{ZWD}_{a}}\cdot m(el^y_a))$$

Model structure

The 4D WV tomography is processed using the Atmospheric Water Vapour Tomography Software 2 (AWATOS 2) which uses a Kalman filter for the forward processing, pseudo-inverse and inter-voxel constraints (Perler 2011). Using a triliniear parameterized field the algorithm of AWATOS 2 expresses the DD SWD observations as a weighted sum of the grid nodes (Perler et al, 2011).

$$\Delta^{SWD} = 10^{-6}\,\Sigma_i \int_{s_i}^{s_i+1} N_{wet,i}\,\Delta s_i$$

The tomography system of equations is solved for wet refractivity using additional constraints in the form of pseudo observations, and optional apriori observations such as radiosonde or ground based meteorological sensors, GPS radio occultation and radiometers. In the matrix form equation with additional information as stated above, reads as follows (Lutz 2008):

$$\begin{pmatrix} \Delta^{2,SWD\,x,y}_{a,b} \\ ZWD_a \\ N_{apriori,i} \\ 0_i \end{pmatrix} = H\cdot\begin{pmatrix} N_{wet1} \\ N_{wet2} \\ N_{wet3} \\ N_{wet4} \\ N_{wet5} \\ N_{wet6} \\ \dots \end{pmatrix}$$

GNSS tomography processing in Australia

This preliminary real data experiment is conducted for 24 hours on the 1st December 2010. GPS data from the Victorian GPS network (Figure 2) was processed using the Bernese GPS processing software V5.0 (Dach et al, 2007).

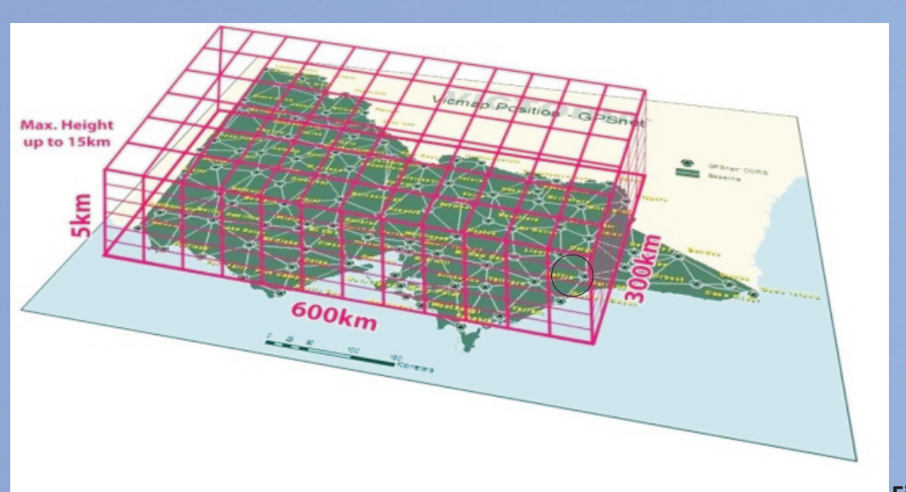

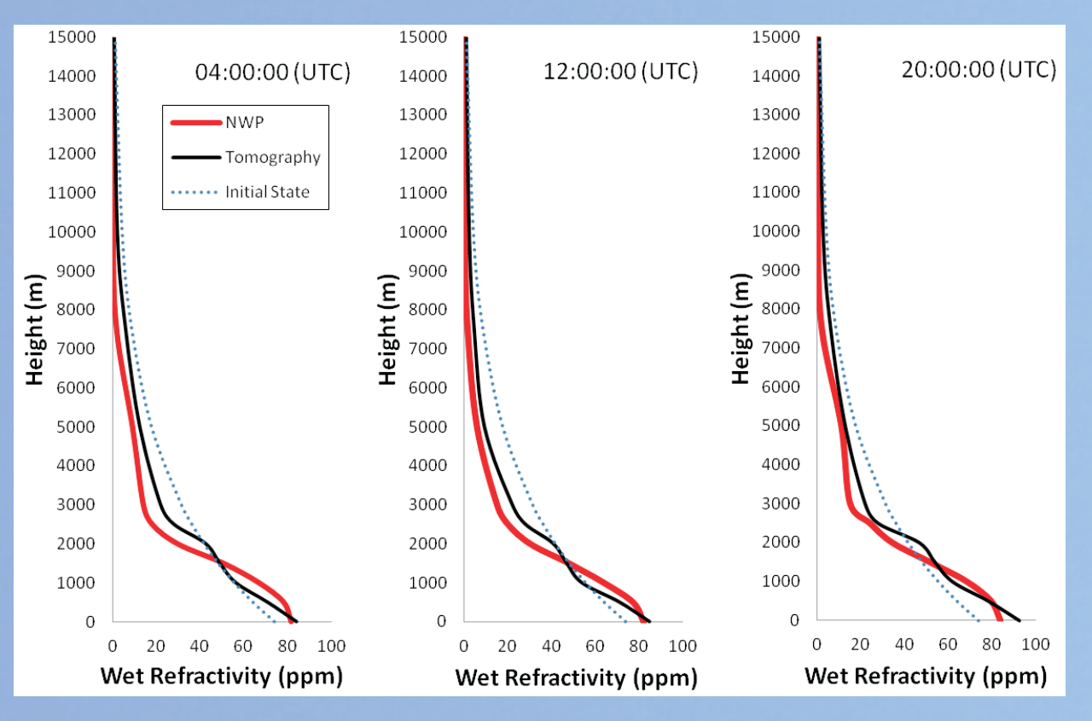

Fig.1. comparison of wet refractivity profiles between NWP and tomographic solution at location (A) presenting 8 hour intervals (04:00:00, 12:00:00, 20:00:00) on 01-12-2010.

Fig. 2. 3D view of the tomographic voxel model showing the first 6 layers

Conclusions on the optimum parameters from the simulation procedure are used for real data processing. A 50km voxel model is used with 15 increasingly larger height layers. This preliminary study restricts the experiment to 1 day with update solutions every 15 minutes. Figure 1 shows the results of an initial profile state and comparison between the tomographic solution and NWP model profiles every 8 hours. Comparisons are quite consistent throughout the campaign with a final RMS of 5.8ppm and a maximum difference of 13ppm. The profiles from the tomography solutions show similar vertical trends as the NWP.

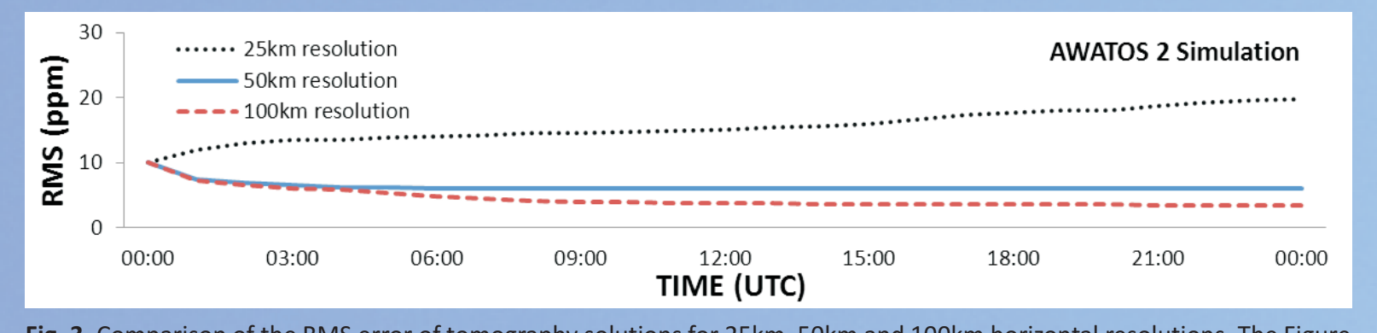

Fig. 3. Comparison of the RMS error of tomography solutions for 25km, 50km and 100km horizontal resolutions. The Figure presents 24 hours of processing. The stabilization of error is evident for 100km and 50km resolutions, whereas, for the 25km resolution we observe an almost linear increase with time.

GFZ

The GFZ hosts an IGS processing center which provides global as well as regional GNSS and tropospheric products in near real-time. The EPOS GNSS processing system estimates ZTDs, IWV and slant total delays (STD), which are used by the GNSS tomography system to reconstruct spatially, resolved humidity fields for Germany:

$$STD = m_h ZHD + m_w[ZWD + \cot\varepsilon(G_N\cos\phi + G_E\sin\phi)] + \delta$$

where ZHD and ZWD are the hydrostatic and wet delay, m_h and m_w are the hydrostatic and the wet mapping function [Niell, 1996; Boehm et al., 2006], G_N and G_E are the delay gradient parameters in north and east, ε is elevation, ϕ is the geographic latitude and δ is the postfit phase residual. The *SWD* is obtained as usual by estimating the *SHD*.

The wet refractivity is discretised on a regular lat/lon/alt grid with an adjustable but equidistant spacing along each axis and assuming a constant refractivity within each voxel (Fig. 1.).

The basic linearised equation:

$$SWD = 10^{-6}\cdot\sum_i N^i_{wet} f(s_i) \;\Rightarrow\; m = An \quad \min\{\|An - m\|\}$$

is solved iteratively by different algorithms of the Algebraic Reconstruction Techniques (ART), e. g. MART

$$n_j^{k+1} = n_j^k\cdot\left(\frac{m_j}{\langle A^i, n^k\rangle}\right)^{\frac{\lambda A_j^i}{\sqrt{\langle A^i, A^i\rangle}}}$$

Additional observations such as synoptic data, radiosonde profiles or integrated quantities provided by water vapour radiometers or the GPS IWV can easily be appended to the set of slant data in order to stabilize the reconstruction.

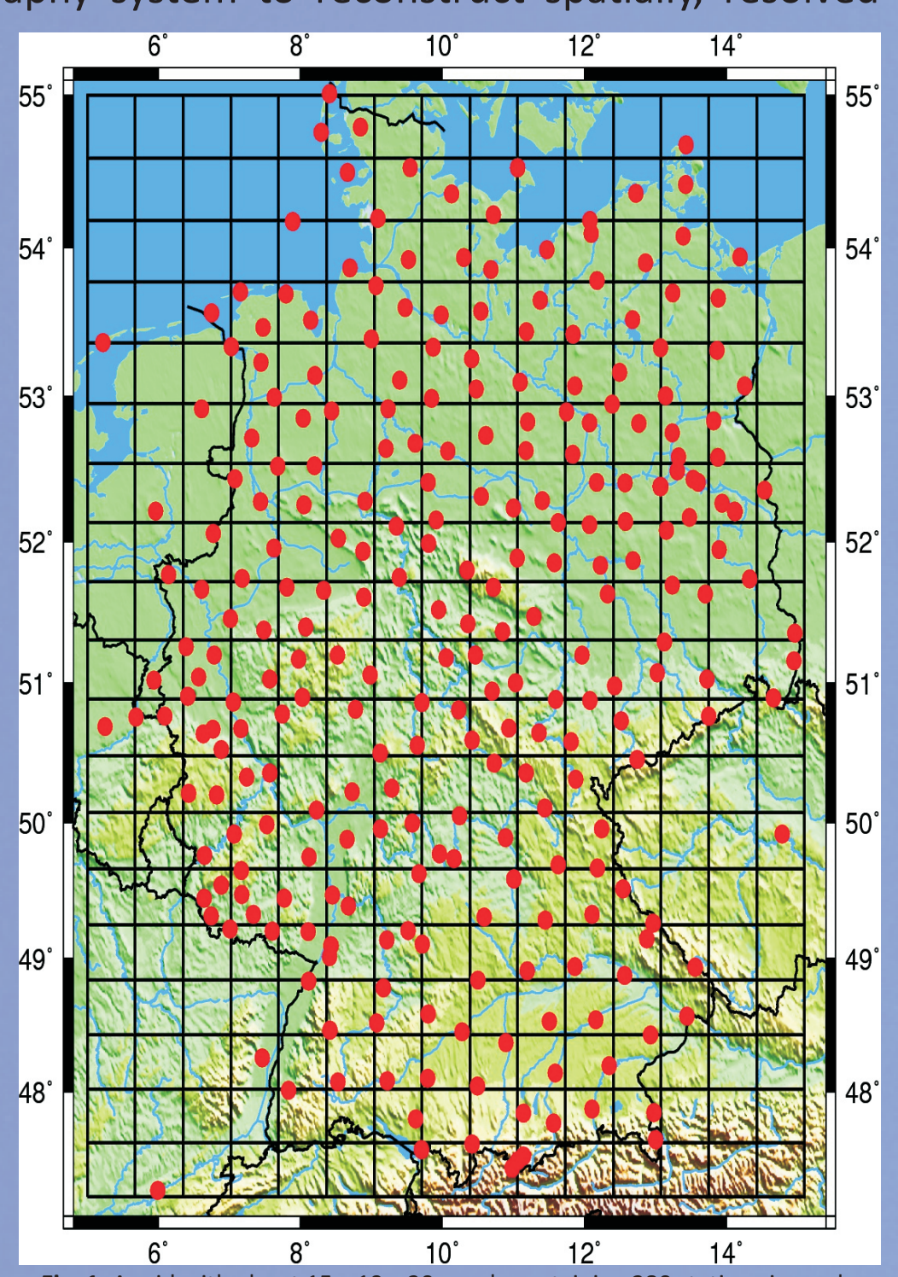

Fig. 1. A grid with about 15 x 19 x 20 voxels containing 280 stations is used by the GFZ.

For Germany the mean interstation distance is about 40 km which defines the upper limit of the horizontal resolution. Vertical resolutions between 200 and 500 m were successfully reconstructed. STDs of all stations are available with an sampling interval of 2.5 minutes but this is in general not sufficient to obtain reliable results. Therefore data from 15 - 30 minutes are combined.

The comparison of tomographically reconstructed humidity profiles with radiosonde profiles shows mostly good results but there is a non negligible fraction of profiles with artifacts, especially in the lower atmosphere and there are regions with insufficient GPS observations.

Recently, the tomography was extended by a Kalman-Filter which can in principle run continuously and "assimilate" the latest observations epoch by epoch. EPOS provides currently hourly batches of STDs with a temporal resolution of 2.5 minutes which are processed in near real-time. Real-time operation with the new EPOS-RT system is possible as soon as the data are available.

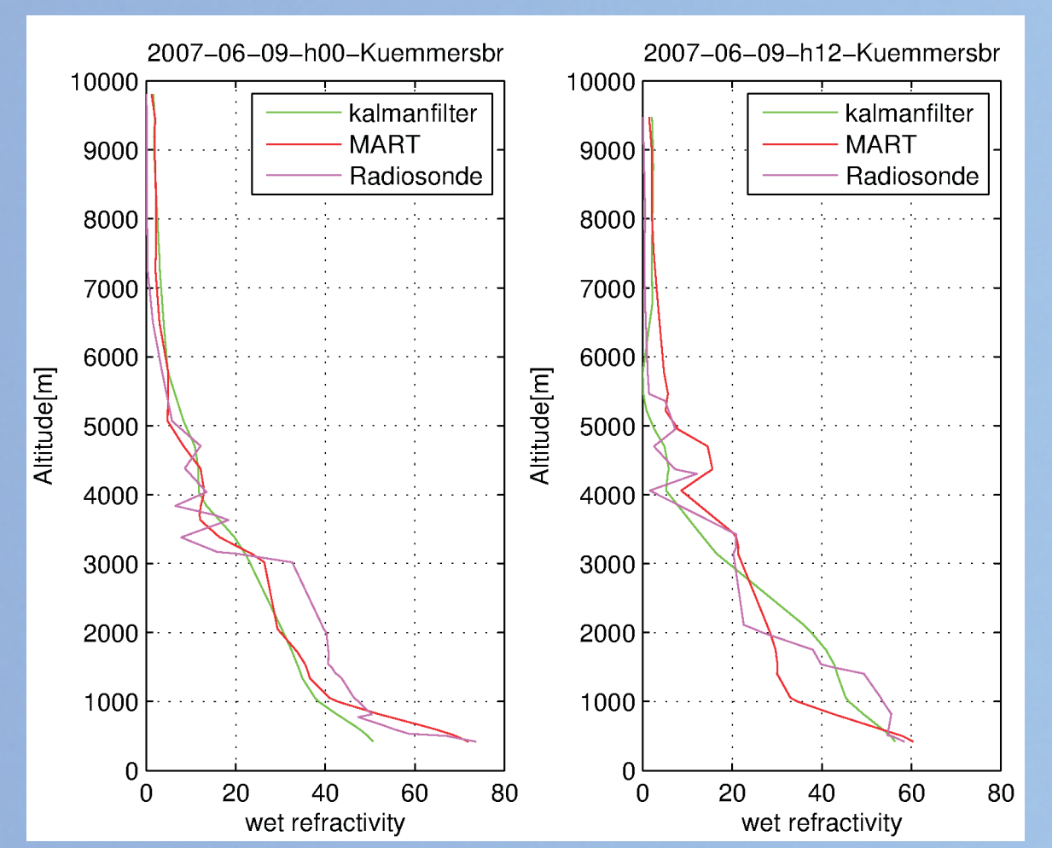

Fig. 2. Validaton between tomography and radiosonde data

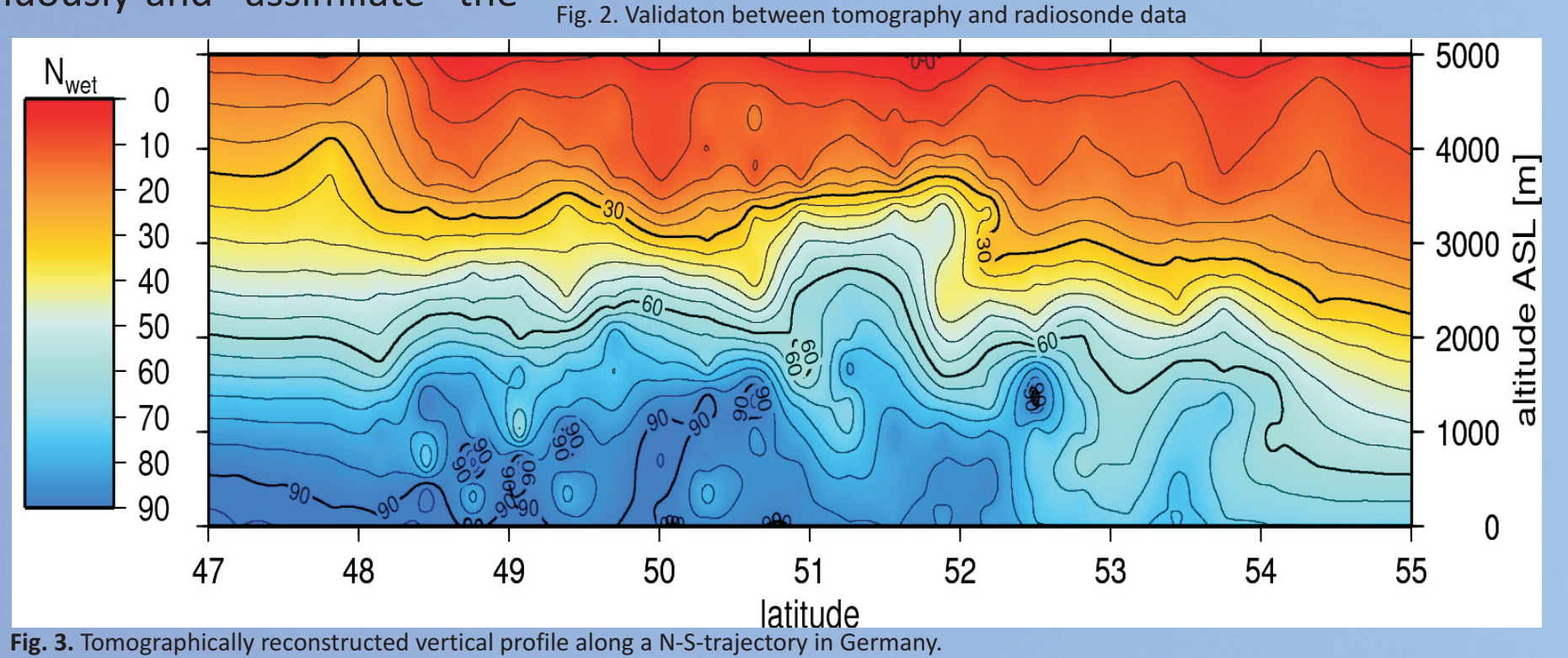

Fig. 3. Tomographically reconstructed vertical profile along a N-S-trajectory in Germany.

LOFFTK MODEL

GNSS meteorology gives continuously Zenith Total Delay measurements of the neutrosphere (ZTD) for any weather conditions. Integrated Water Vapour contents (IWV) can be converted from ZTD using ground pressure and temperature. Using mapping function (Boehm et al., 2006) and slant IWV, GNSS tomography can allow to resolve the spatial structure and temporal behaviour of tropospheric water vapour. We use at BIRA an adaptation of the LOFFTK developed by Champollion et al. (2009).

GNSS tomography can be limited to network geometry, initial conditions and accuracy of slant IWV (not treated in this study).

Overview of our tomographic process:

A Singular Value Decomposition (SVD) is used in our tomographic software, to estimate the generalised inversion of the rectangular matrix G. The dimension of the cell we used is 0.1 ° width (~ 10 km) in horizontal and 500 m in vertical.

Linear inverse problem: $d = Gm + C_D$

where *d* data, *G* geometrical matrix, *m* model solution, C_D covariance operator data.

Mixed invert problem (under- and over-determined): $m = \cancel{G^{-1}}d + C'_D$

$$m = m_0 + (G^t C_D^{-1} G + C_M^{-1})^{-1} G^t C_D^{-1}(d - Gm_0)$$

where m_0 apriori model, C_M covariance operator apriori model. We apply the covariance operator of data (C_D) of 10% and covariance operator of a priori model (C_M) of 90 %.

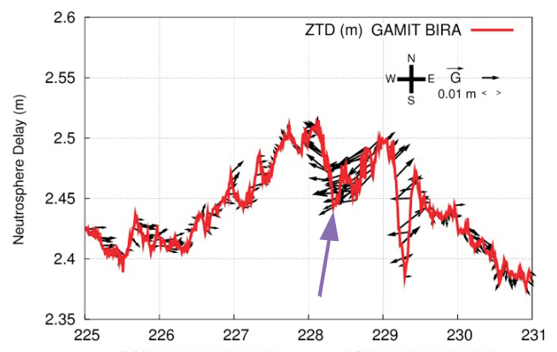

Fig.1. Time-series of ZTD and gradients from GAMIT

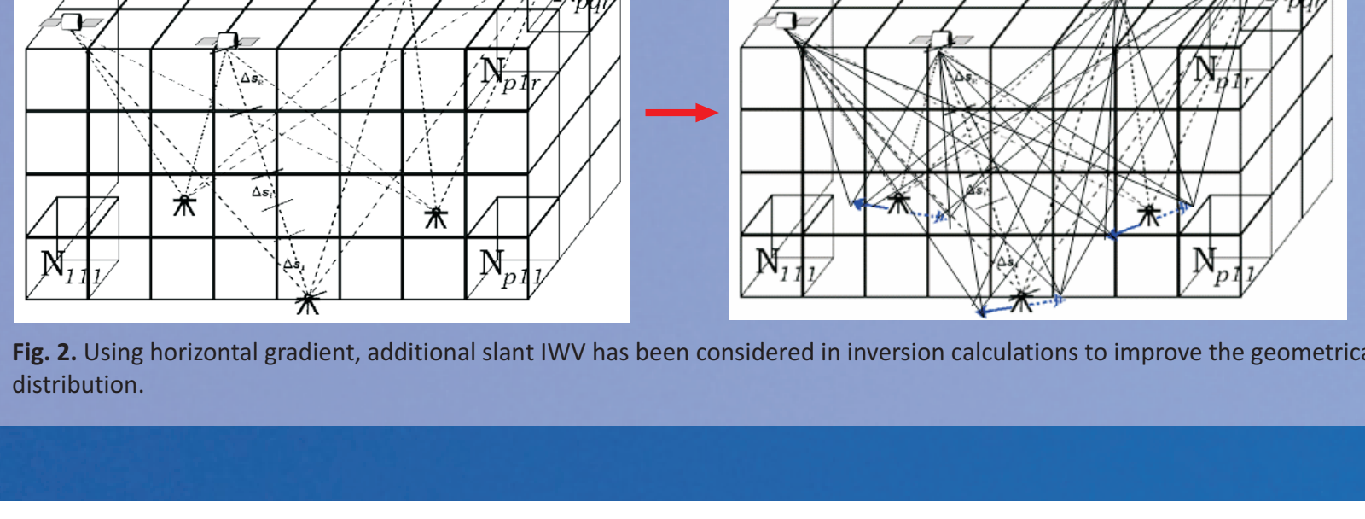

Fig. 2. Using horizontal gradient, additional slant IWV has been considered in inversion calculations to improve the geometrical distribution.

Atmosphere based on ALARO model + GNSS tomography gradient improvement.

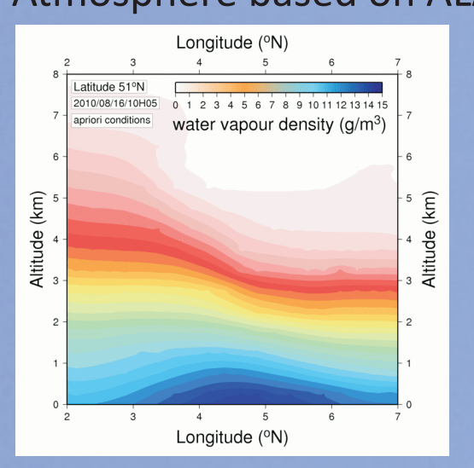

Fig. 3. A priori model

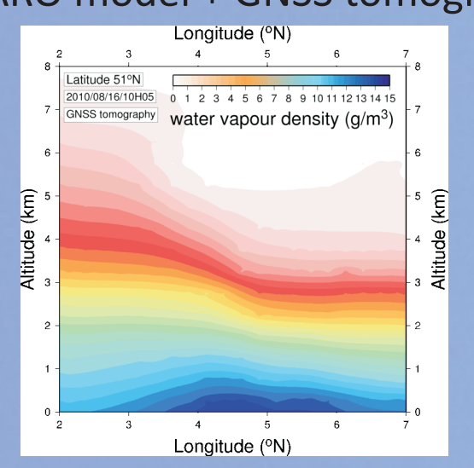

Fig.4. GNSS tomography

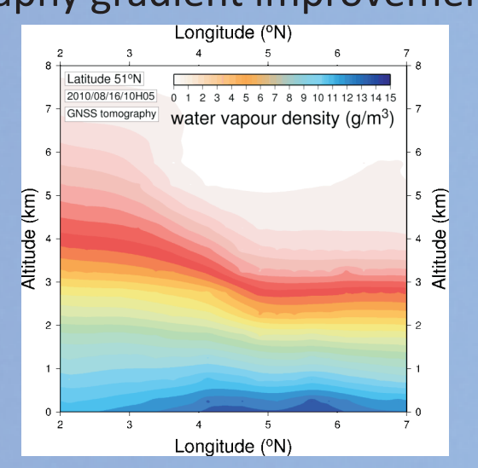

Fig. 5. GNSS tomography with gradient improvement

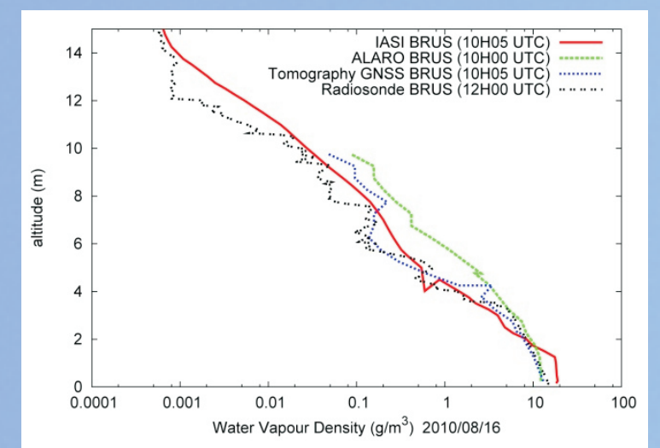

Fig. 6. Water vapour density profiles from IASI, ALARO model, radiosonde, GNSS tomography, and GNSS tomography with gradient improvement.

Conclusions:

- 2D field of IWV improved GNSS gradients,
- comparison of IWV from IASI, ALARO and GNSS for several events and special interest of GNSS for nowcasting,
- sensitivity of tomography to initial conditions,
- gradient observations and positive impact on geometrical matrix and water vapour density adjusted by GNSS tomography,
- GNSS tomography using initial conditions from NWP & interest for nowcasting.

Perspectives:

1. Improvement of the resolution of our water vapour retrievals
   - increase horizontal resolution,
   - use of a Kalman filter to improve geometrical resolution,
   - use of special covariance operator.
2. Operational IWV observations for the Belgian Dense Network and tomography retrievals for nowcasting.

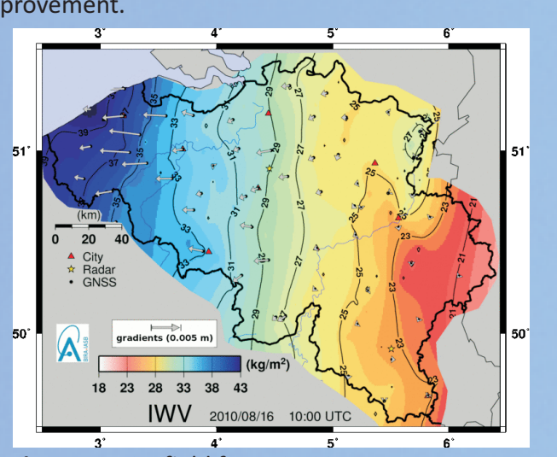

Fig.7. IWV 2D field from GNSS.

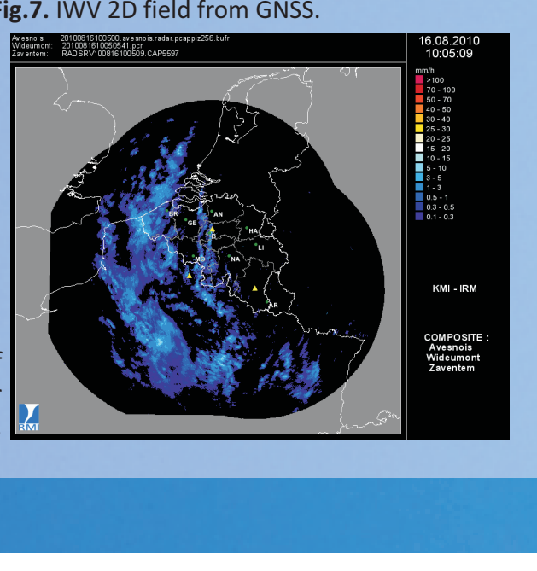

Fig.8. Radar precipitation of this depression coming over Belgium, 16/08/2010 at 10:00 UTC.

SCOPE

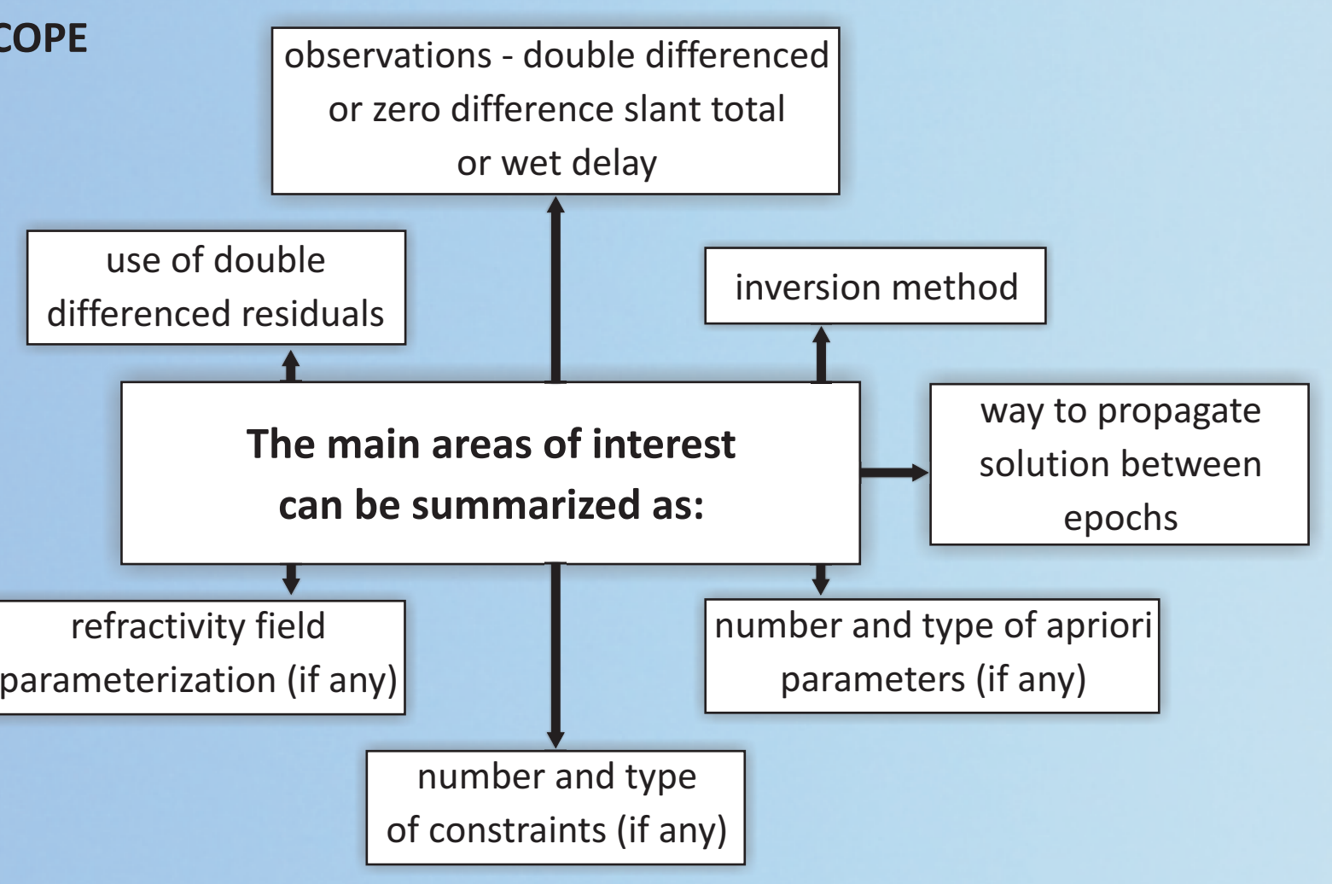
The main areas of interest can be summarized as:
observations - double differenced or zero difference slant total or wet delay
use of double differenced residuals
inversion method
way to propagate solution between epochs
refractivity field parameterization (if any)
number and type of apriori parameters (if any)
number and type of constraints (if any)

CHALLENGES

1. Inclusion of other than GNSS ground based observations in the tomography equation (space based)
2. Improvement in STD and SWD estimation methods
3. Applying robust estimation algorithms to observations to limit the noise influence and remove outliers
4. Derivation of consistent precision and accuracy measures
5. Switching to NRT mode
6. Interoperability with NWP models

METHODS

Best practice in GNSS STD and SWD PPP and DD estimation along with DD residuals

↓

Reliable reference data – NWP, radiosonde, RO, radiometer, ground based

↓

STD and SWD accuracy and precision studies

↓

Harmonized voxel horizontal and vertical extent

↓

Case studies to reveal strong and weak points of models

↓

Cooperation with NWP community to include GNSS tomography models as one of data in assimilation step

TOOLS

data exchange ftp server
hosted by : igig.up.wroc.pl

mailing list

shared documents directory to work online
IAGtomography@gmail.com

REFERENCES

TOMO 2

Bosy J., Rohm W., Sierny J. *The near real time atmosphere model based on the GNSS and the meteorological data from the Ground Base Augmentation System ASG-EUPOS* International Archives of the Photogrammetry, Remote Sensing and Spatial Information Science, Vol. XXXVIII No. 8, Kyoto, Japan 2010, pp. 366-371

Rohm W. *The precision of humidity in GNSS tomography* Atmospheric Research, Vol. 107 No. , 2012, pp. 69-75

Rohm W., Bosy J. *The verification of GNSS tropospheric tomography model in a mountainous area* Advances in Space Research, Vol. No. , 2011, DOI: 10.1016/j.asr.2010.04.017

Rohm W., Bosy J. *Local tomography troposphere model over mountains area* Atmospheric Research, Vol. 93 No. 4, 2009, pp. 777-783,

AWATOS2

Lutz, S.; Troller, M.; Perler, D.; Geiger, A.; Kahle, H.-G., 2010. *Better Weather Prediction Using GPS*, GPS-World, Vol. 21, No. 7. 40-47.

Perler. D. (2012) *Water Vapor Tomography using Global Navigation Satellite Systems*. Swiss Geodedic Commission, Vol 84. P. 188. ISBN 978-3-908440-30-7. (http://www.sgc.ethz.ch/publications)

Perler, D., A. Geiger, and F. Hurter (2011). *4D GPS water vapor tomography: New parameterized approaches*, Journal of Geodesy, Springer, DOI: 10.1007/s00190-011-0454-2.

Troller, M., Geiger, A., Brockmann, E. and H.-G. Kahle, 2006. *Determination of spatial and temporal variation of tropospheric water vapor using CGPS networks*. Geophys. J. Int. 167(2):509-520, doi:10.1111/j.1365-246X.2006.03101.x.

GFZ MODEL

Bender, M.; Dick, G.; Ge, M.; Deng, Z.; Kahle, J. W. H.-G.; Raabe, A. & Tetzlaff, G., *Development of a GNSS Water Vapor Tomography System Using Algebraic Reconstruction Techniques*, Advances in Space Research, 2010, 47, 1704-1720

LOFFTK

Champollion C., Drobinski, P., Haeffelin, M., Bock, O., Tarniewicz, J., Bouin, M.-N., and Vautard, R.: *Water vapour variability induced by urban/ruarl surface heterogeneities during convective conditions*, QJRMS, 135, pp. 1266-1276, 2009.

Brenot, H., Champollion, C., Deckmyn A., van Malderen, R., Kumps, N., Warnant, R., and De Mazière, M.: *Humidity 3D field comparisons between GNSS tomography, IASI satellite observations and ALARO model.* Oral presentation, vol. 14, EGU2012-4285, 2012.

Brenot, H., Neméghaire, J., Delobbe, L., Clerbaux, N. and Van Roozendael, M.: *Preliminary signs of the initiation of deep convection by GNSS.*, ACPD, 2012. (this paper is in minor review and will on ACPD at the end of July during thr IGS worshop).

INTERESTED IN GNSS TOMOGRAPHY? WANT TO JOIN THIS WG?
contact us on:

- alain.geiger@geod.baug.ethz.ch
- witold.rohm@igig.up.wroc.pl